Soil Water Characteristic Curve for a Residual Granite Soil

Mehrdad Kholghifard[1*], Kamarudin Ahmad[2]

[1]Department of Civil Engineering, Yas.C., Islamic Azad University, Yasuj, Iran

[2]Department of Geotechnics and Transportation, School of Civil Engineering, Universiti Teknologi Malaysia, UTM, 81310 Johor, Malaysia

*Corresponding author's email: kholghifard.m@iau.ac.ir

Abstract:
Soil-water characteristic curve (SWCC) is one of the important keys for estimating the behavior of unsaturated soils. The aim of this study was to establish SWCC of the residual granite soil in laboratory. Therefore, a modified oedometer based on the axis translation technique successfully employed to perform various experiments in unsaturated condition. Soil water characteristic curve (SWCC) for a residual granite soil at different densities was then established based on results obtained from experiments using the oedometer. Results showed a good trend between the experimental and numerical methods, verifying the established SWCC. Finally, an empirical equation was established to describe relationship of the granite soil water characteristic curve (GSWCC) as it fitted well with the experimental results.

Keywords: SWCC, residual granite soil, suction

1. Introduction

Tropical residual soils from Malaysia have some problematic features as high void ratio, low natural dry density, suction changes due to drying and wetting in unsaturated part of the soil above ground water level and loose of apparent cohesion of the soil immediately after rain due to wetting or suction reduction

[1, 2]. All the factors mentioned above are very significant and effective on the mechanical behavior of the residual soil. The relationship between volumetric water content (θ_w) and matric suction (s or ψ) is called soil-water characteristic curves (SWCC). The difference between the air pressure (u_a) and the water pressure (u_w) in an unsaturated soil sample is known as matric suction and expressed as ($u_a - u_w$). The principle of an experimental device for the measurement of matric suction in unsaturated soils using the axis translation technique is the measurement of a differential pressure across a high air entry value (HAVE) ceramic disk [3].

SWCC was studied as an important key in the behavior of unsaturated soils by several researchers [4, 5]. The importance of the SWCC is not only in giving insight into soil-water interaction but it is also used to measure the hydraulic conductivity, water volume change, shear strength, swelling, and collapsibility which are subsequently needed to estimate the unsaturated soils behavior [6, 7, 8]. In fact, the SWCC of a soil is the key function when dealing with unsaturated soils [6]. Figure 1 shows a typical SWCC in their stages during drying path, the capillary saturation, desaturation or transition and residual stages. Similar stages can be identified for the wetting phase. There are also two distinct changes in slope along the SWCC. The changes in slope define two points that are fundamental to describing the SWCC. The first point is termed the ‘‘air-entry value’’ of the soil, where the largest voids start to desaturate as suction is increased. The second point is termed ‘‘residual condition’’ where the removal of water from the soil becomes significantly more difficult (i.e., requires significantly more energy for water removal).

During capillary saturation zone, soil remains nearly fully saturated. This zone is immediately located above the water table. The pore water pressure is negative and the soil is in saturated state due to capillary. At the ‘‘air-entry value’’ point, the applied suction is higher than the capillary forces and the air starts to enter the soil pores. The air entry value of soil depends upon the soil type and grain size. Various soils have different air entry value. The zone located before this point is known as the saturation zone. Beyond the air entry value point, the desaturation zone begins. As the degree of saturation is decreased, the suction is sharply increased and the water void in the soil is displaced by the air void. In the last stage

or residual saturation zone, water is tightly adsorbed into the soil particles and soil is mostly considered in a dry condition.

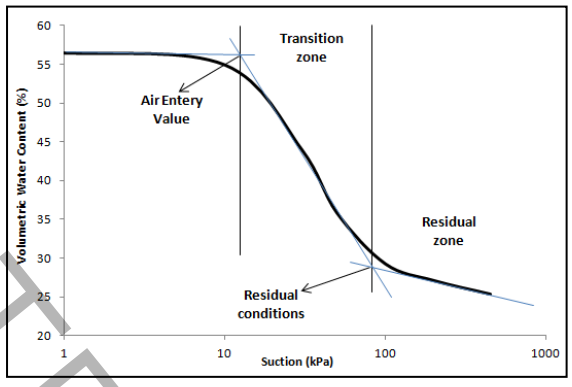

Fig. 1. Stages of SWCC for an unsaturated soil

The SWCC has been widely studied and many empirical mathematical expressions have been proposed to describe a single soil-water characteristic curve in drying path by researchers [9-13]. An important feature of the water retention curve is the hysteresis observed between drying and wetting behavior.

To study hydromechanical behavior of unsaturated soil, pressure plate devices were developed based on the axis translation technique (ATT). Despite these advances, some problems such as evaporation and condensation of water on the cell wall are still reported, which causes errors in the calculation of water volume change. In this study, a modified suction-temperature-controlled oedometer was employed that allows testing of the complete SWCC on a single specimen without dismantling the device. It also allows a combination of controlled suction and temperature is applied on the soil sample indirect way, causing a uniform temperature into the soil sample. Consequently, the water volume error is reduced. On the other hand, soil-water characteristic curve (SWCC) of residual granite soil in laboratory using the modified oedometer is established with lowest errors. Therefore, the aim of this research is to study soil-water characteristic curve (SWCC) of a residual soil in laboratory using a modified suction-temperature-controlled oedometer whiteout any problem related to water condensation. To achieve this, an odometer is first modified to perform SWCC tests with minimal error. Then software simulation is employed to verify

the test results. Finally, an experimental relationship was proposed to describe the SWCC by fitting two well-known relationships on the laboratory results.

Materials and research methodology

2-1- Soil sampling

In this study, a ground investigation was conducted to identify engineering properties and structural elements of the residual soil. Data from sampling points were analyzed to determine the physical and engineering properties of the soil.

The results indicated that the profile from 1.5 to 2.5 m of depth (passing through the topsoil layer, roots of trees and plants, also achieving natural soil condition) was composed of a reddish-brown residual soil of Grade VI [14, 15,16]. By collecting samples in the region, the natural density of samples was around 85% (loose) to 95% (dense). Figure 2 shows the particle size distributions of the residual soil. To determine the type and number of major elements, clay minerals and non- clay minerals, Scanning Electron Microscope (SEM) imagery and Energy Diffraction Analysis of X-rays (EDX) were performed on the selected samples of the residual soil (Figures 3 and 4). Table 1 shows the soil properties and EDX analysis used to identify the elemental composition of the granite residual samples. The results indicated that the samples consisted of magnesium, aluminum, and iron compounds. SEM of the granite residual soil was indicated a porous structure.

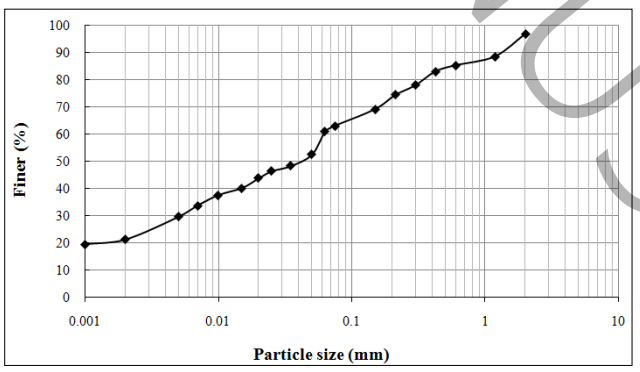

Fig. 2. Particle size distribution of the soil

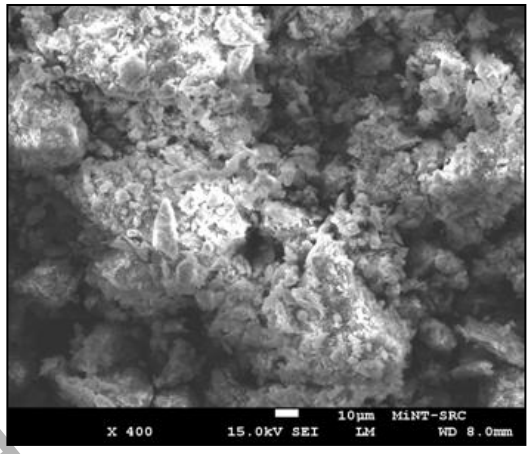

Fig. 3. SEM images of the soil

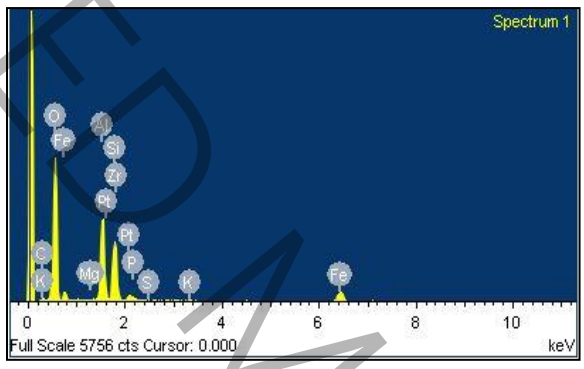

Fig. 4. EDX spectra of the residual soil

Table 1. Basic properties of the granite residual soil

Indices	Value
Liquid limit, LL (%)	68
Plastic limit, PL (%)	35
Plasticity index, PI (%)	33
Properties	
Optimum moisture content, OMC (%)	30
Maximum dry density, MDD (Mg/m3)	1.42
Specific gravity, G_s	2.67
Natural dry density (Mg/m3)	1.21
Natural water content, w_n (%)	27
Elements	
MgO (%)	0.12
Al_2O_3 (%)	36.53
SiO_2 (%)	37.03

Fe_2O_3	26.32

2-2- Modified oedometer with control suction and temperature

According to literatures related to application of the axis translation technique (ATT) and ASTM D6836-02 [17] a new modified oedometer for performing consolidation test on unsaturated soil with control suction and temperature was fabricated. The modification was conducted on a conventional oedometer so that the improved device can be employed for consolidation test under saturated and unsaturated conditions. Such oedometer device allows for testing of the complete SWCC on a single specimen without dismantling the device. It also allows a combination of controlled suction and temperature to obtain SWCC and consolidation test on unsaturated soil sample. Assembled system of the modified oedometer is shown in Figure 5.

In order to measure the temperature and minimize evaporation on the cell wall during the tests, the oedometer device was also customized with a temperature chamber which was connected to a thermo-controller unit with accuracy of ±1 ºC. The external cell was designed such that heated water covered the entire internal air tight cell. High air entry value (HAEV) ceramic disk has been designed to prevent the passage of air bubbles. In this device, a 1500 kPa ceramic disk was used, which allows applying level of suction up to 1500 kPa. A data logger connected to a computer continually recorded vertical stress, air pressure, water pressure, and vertical displacement. For monitoring and controlling the variants during test, two consolidation and triaxial cods of DS7 software [18] were combined and modified for the modified oedometer. Before conducting any test, the modified oedometer and other equipment connected to the system were calibrated based on ASTM and suggestions by Fredlund and Rahardjo [19].

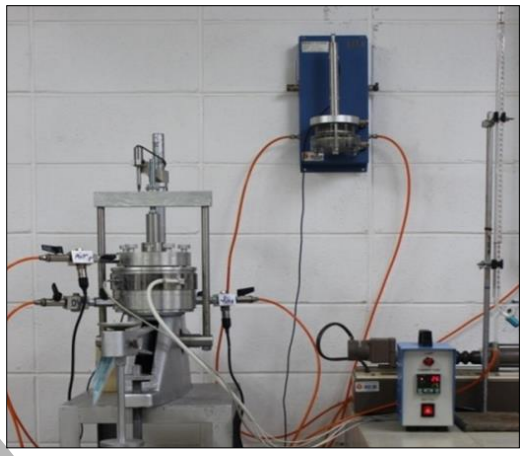

Fig. 5. Assembled system of the modified oedometer

2-3- Laboratory test using modified oedometer

Prior to performing any test using the modified oedometer system, it is necessary to calibrate the modified oedometer system. The soil samples were prepared in two groups: LS (loose soil) group with 85% relative compaction degree and DS (dense soil) group with 95% relative compaction (20 mm height and 75 mm diameter). Then they fully saturated in 24 hours. The degree of saturation was ensured from mass-volume relationships. Initial conditions of the soil samples are shown in Table 2. Prior to performing any test using the modified oedometer system, it is necessary to saturate the ceramic disk and flush air bubbles from the water compartment.

To define SWCC of the unsaturated granite residual soil, the saturated LS and DS samples were subjected to several prearranged suction steps using axis translation technique. All the tests were begun at water saturated conditions. Then, the samples were subjected to a number of prearranged suction steps using the axis translation technique. For drying tests, suction pressure was increased from zero (saturated) to 700 kPa in steps of 5, 10, 25, 50, 100, 200, 400, 500, and 700 kPa. The suction in the sample was increased in several steps, by increasing the air pressure on the top of the sample and holding the water pressure constant at zero kPa beneath the sample. The volume of water expelled at each step was measured using a GDS pressure system. The time required to achieve this result varied from 1 to 4 days. The equilibrium time depends on the soil permeability, matric suction value, initial water content of the soil sample, as

well as the thickness of the ceramic disk. Then, the volumetric water content (θw) of the soil sample was calculated using Equation 3 [20] for each step.

Table 2. Initial conditions of the soil samples for SWCC tests

Type of Soil	**LS**	**DS**
Void ratio	1.207	1.03
Dry density, (gr/cm3)	1.21	1.35
Water content (%)	43.1	35.2
Degree of Saturation (%)	100	100
Suction(kPa)	0	0

$$\theta_w = \frac{wG_s}{1+e_0} \quad (1)$$

Where, θ_w= volumetric water content, w = water content in percent (or gravimetric water content), G_s= specific gravity of soil particles and e_0 = initial void ratio. To investigate the problem related to water condensation, SWCC test for the LS residual granite soil was repeated while the modified device dismantled at the end of each applied suction (10, 50 100, 200, 400 and 700 kPa) and the water content directly determined by weighing the sample. To minimize water condensation on the cell wall, the SWCC test for the soil samples were also conducted using the modified oedometer with heating control system at temperature of 30 ºC.

Fredlund and Xing [9] equation and Van Genuchten [10] equation appear to be the most commonly used continuous function for a SWCC as follows respectively:

$$\theta = \theta_s\left[1-\frac{\ln(1+\psi/\psi_r)}{\ln(1+10^6/\psi_r)}\right]\left[\frac{1}{\{\ln[e+(\psi/a)^n]\}^m}\right] \quad (2)$$

$$\theta = \theta_r + \frac{(\theta_s-\theta_r)}{[1+(b\psi^p)]^q} \quad (3)$$

Where θ = volumetric water content, θ_s= saturated volumetric water content, θ_r= residual volumetric water content, ψ = matric suction (kPa), ψ_r= matric suction at residual water content (kPa), e=2.71828; base of natural logarithm, a, b, m, n, p and q are fitting parameters that describe the shape of SWCC. SWCC for different types of soils differ from each other depending on the structure or arrangement of the

soil particles, the grain-size distribution, pore-size distribution as well as the density. Therefore, SWCC of granite residual soils might have a different relationship. These empirical models are essentially curve fitting equations, established through best fit on test data.

2-4- Numerical simulation of the modified oedometer for SWCC test

The main objective of numerical simulation was to verify the results obtained from the modified oedometer. In addition, the modelling was employed to identify variations of other parameters such as suction, water content, water flow (flux or water volume change) and hydraulic conductivity. Hence, a coupled air-water transfer analysis was performed using the GeoSlope software. This software is a powerful software in geotechnical engineering matters especially in simulation of unsaturated soil conditions. Besides, GeoSlope software has various modules that are used for different analysis: SIGMA/W, SLOPE/W, SEEP/W, QUAKE/W, TEMP/W, AIR/W, CTRAN/W, VADOSE/W. This software can employ a coupled SEEP/W and AIR/W code to model water flow (seepage) in the unsaturated soil based on numerical simulation [21]. This code was used to simulate the SWCC test in the modified oedometer cell. Schematic of the oedometer cell and the corresponding model geometry are shown in Figure 6.

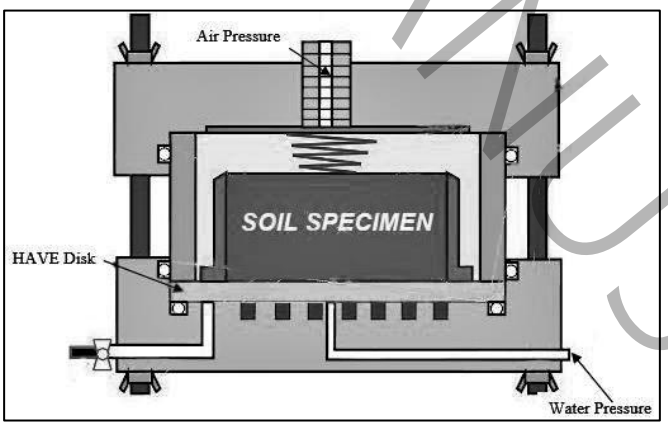

Fig. 6. Schematic of the oedometer cell

The model of the residual granite soil samples was prepared in two groups (LS and DS) with 75 mm diameter and 20 mm thickness and placed above the disk. A pore-water pressure head of 0.01 m (10

mm) was applied to the bottom of the ceramic (10 mm thickness), which establishes a zero-pressure condition at the base of the sample. An air pressure of 0 kPa was applied to the top, right and left edges of the sample such that atmospheric conditions established through the sample at the start of the analysis. Then, the drying stage analysis were performed by applying incremental air pressure (10, 25, 50, 100, 200, 400,500 and 700 kPa) on the top and sides (right and left edges) of the sample in a transient state analysis. For each incremental air pressure, the soil is allowed to drain. The cell was considered such that the positive air pressure was applied at the top. Water could expulse from the sample and collect beneath the HAEV disk. All drained water was collected and the total volume of water leaving the sample was calculated. At each stage, when the drainage stopped, a new air pressure was applied to drive more water out. It was important to allow full drainage before incrementing the applied air pressure. The small-time steps were considered such that rapid changes in air pressure and water pressure could be captured by the analysis. Based on the engineering manual of GeoSlope software [21], simulation of a three-dimensional problem can be made using an axisymmetric analysis with symmetry around a vertical axis of rotation (Figure 7). A steady state coupled air-water analysis was used to establish the initial conditions. In the following process, a transient state was considered. Initial properties of the residual soil used in the region above the ceramic (such as: saturated hydraulic conductivity,K_{sat}, saturated volumetric water content, θ_s, air entry value, s_{ae}, coefficient of volume change, m_v, and specific gravity, G_s) are presented in Table 3. Before simulation of the model, finite element mesh was generated for the whole region. The number of mesh used in this model was designed as 360 (30 x 12) including the soil and ceramic. A period of 2 to 5 days was set for each step in the analysis. The small-time steps were considered such that rapid changes in air pressure and water pressure could be captured by the analysis.

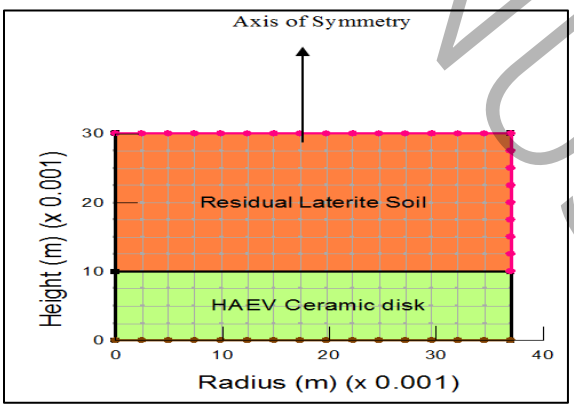

Fig. 7. Geometry information and boundary conditions

Table 3. Properties of the materials used in numerical simulation

Type of soil	LS	DS

θ_s (m3/m3)	0.519	0.47
s_{ae} (kPa)	11	20
θ_r (m3/m3)	0.276	0.29
K_{sat} (cm/sec)	5.1 x 10-5	3.1 x 10-5
m_v (1/kPa)	3.2 x 10-4	2.05 x 10-4
G_s	2.67	2.67

2. Results and discussion

3-1- SWCC resulted from the modified oedometer

The SWCCs in terms of volumetric water content versus matric suction resulted from the modified oedometer are shown in Figure 8 for both LS and DS soils, respectively. Based on the SWCC, the unsaturated parameters such as saturated volumetric water content (θ_s), air entry value (s_{ae}), residual suction (s_{res}) and residual volumetric water content (θ_r) of the soil samples were determined as presented in Table 4.

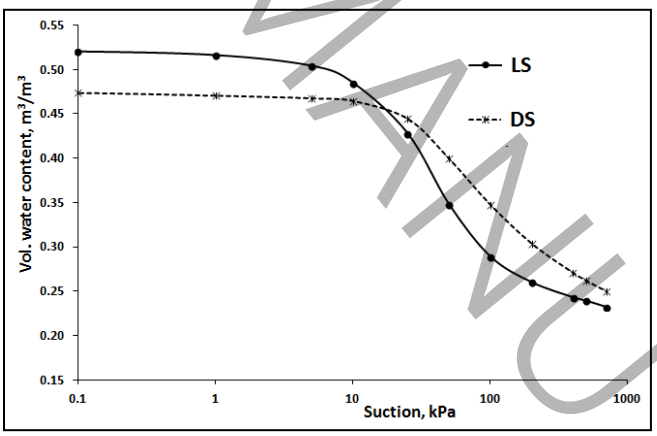

Fig. 8. SWCCs, LS and DS

Table 4. SWCC parameters for the LS and DS soils

Type of soil	LS	DS
θ_s (m3/m3)	0.519	0.474
s_{ae} (kPa)	11	20
θ_r (m3/m3)	0.276	0.29
s_{res} (kPa)	88	213

The LS soil with a higher pore volume indicated higher degree of saturated volumetric water content (51.9%) than that of the DS soil (47.4%). This verified a wider range of pore size distribution for the LS soil compared to the DS soil. In contrast, the LS soil had a lower level of air entry value of 11 kPa compared to the DS soil with 20 kPa. The wetting curves of SWCC showed lower volumetric water content values at saturation point than the drying curves due to entrapped air in the pores. As a result, the s_{ae} of the LS soil with lower degree of compaction was very low (11 kPa). On the other hand, the DS soil with higher degree of compaction had the ability to maintain water under high level of suction due to small pores. Hence it caused a higher s_{ae} for the DS soil (20 kPa). This difference in volumetric water content behavior may be attributed to the smaller pore sizes that exist in DS soil as compared to LS soil. Generally, the results indicated that the particle size distribution and initial void ratio are reflected in the SWCC shape of the residual soils [22].

Generally, results showed that the water pressure increased up near to the air pressure during the drying paths at the start. The low conductivity of the soil samples caused the pore-water pressure slowly dissipated specially for the DS soil. As a result, water was drained out slowly from the base of the samples through the HAEV ceramic. It was noticeable that the water flow into the sample from below was controlled by the hydraulic conductivity of the ceramic and the soil samples. The pore water pressure dissipation was faster in the LS soil sample compared to DS at each step of applied suction due to higher hydraulic conductivity of the LS soil than that of the DS soil. As a result, the DS soil required more time to complete a drying-path than the LS soil.

3-2- Numerical simulation result for SWCC

The most significant parameter in the simulation of unsaturated soil is the amount of water flow out or into the model as shown in Figures 9 and 10. The velocity vector and pore air pressure are also presented in Figure 9. The water content decreased due to dissipation of the pore water pressure during drying path, while the air content increased by the same amount. From the graphs (Figure 10), the DS model requires more time to complete a whole drying-wetting process compared to the LS model, which is within close

agreement to the experimental results. The drying-wetting process in this case was not completely reversible for both models. At the end of the wetting path, 7.81 cm3 and 8.58 cm3 of water did not flow back into the LS and DS models, respectively. This means that hydraulic hysteretic effects had an impact on both the LS and DS soils.

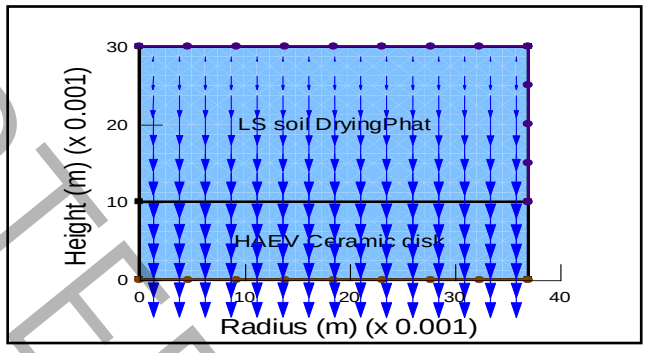

Fig. 9. Pore air pressure counter and velocity vector

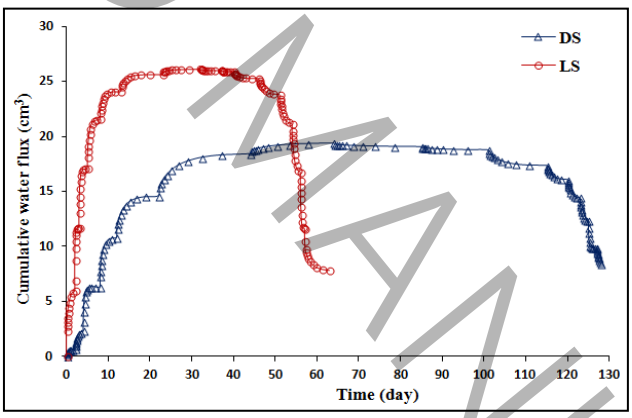

Fig. 10. Cumulative water flux, LS and DS

3-3- Comparison of numerical and experimental methods

The SWCCs calculated based on the amount of water flow during a drying-wetting cycle for both models (the LS and DS) obtained from Geo-Slope fitted and experiments are presented in Figure 11 and Figure 12. In fact, the figures show SWCCs obtained from experimental results and numerical results. The figures also show that the LS soil comprises higher water retention capacity than the DS soil in both methods. The range of air entry values for the LS and DS obtained in the experiments were found approximately similar to the results obtained from the numerical simulation. The maximum differences in

the values of volumetric water content obtained from the experimental and numerical methods were about 5.7% for the LS and around 3.5% for the DS. As a result, the experimental and numerical results showed a similarity of about 95% to 97%. The SWCC results obtained from the experimental indicated similar trend to the results from GeoSlope showing that the results obtained from the modified oedometer are reliable in unsaturated condition (Figures 11 and 12). Earlier works by other researchers indicated that the difference in volumetric water content between experimental and numerical methods were less than 10% [23].

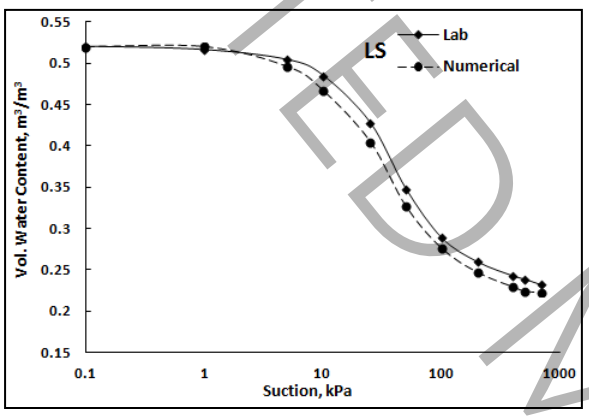

Fig. 11. Experimental and numerical SWCCs, LS

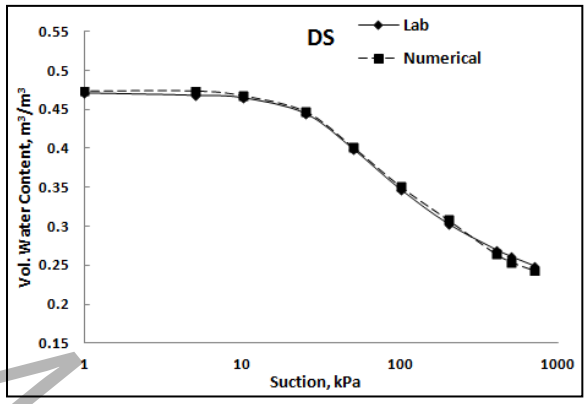

Fig. 12. Experimental and numerical SWCCs, DS

3-4- Empirical equations for SWCC of the granite soil

SWCC has been extensively studied and many empirical mathematical expressions have been proposed to describe a single (primary drying) soil-water characteristic curve [e.g. 24, 25, 26, 27]. Most of the required hydromechanical behavior data is obtained from the dry path. The most common models were developed by van Genuchten (1980) and Fredlund and Xing (1994) as described in equations 2 and 3, respectively. These empirical models are essentially curve fitting equations, established through best fit on test data. Most of them ignore hysteresis effects.

In this study, the Eqs (1) and (2) were employed to fit on the experimental results [28] as shown in Figures 13 and 14, respectively. The SWCC parameters obtained for the LS and DS soils are presented in Table 5. As can be seen from the figures, the laboratory experimental curve developed using the equation of Fredlund and Xing is almost perfectly line on the laboratory data especially at high suction pressure

(more than 100 kPa). From Table 5, the air entry values of Fredlund and Xing fitting (9.57 and 18.96 kPa) are very close to the air entry values obtained from laboratory data (11 and 20 kPa for) the LS and DS soils respectively, compared to the Van Genuchten data. Regarding residual water content, the Fredlund and Xing values (29.2 and 28.7 kPa) are also more reasonable compared to the value of Van Genuchten. The Coefficient of determination parameters (R2) for both the DS and LS imply that the Fredlund-Xings [9] equation is a tight-fit to the laboratory data. Consequently, modified of equation 3 proposed by Fredlund and Xing [9] can well be employed to fit on SWCC of the residual granite soil as bellow:

$$\theta = \theta_s \left[1 - \frac{\ln(1+\psi/\psi_r)}{\ln(1+10^6/\psi_r)}\right]\left[\frac{1}{\{\ln[e+(\psi/a)^n]\}^m}\right], 11 \le a \le 15, 1.7 \le n \le 2.3, m = 0.4 \quad (4)$$

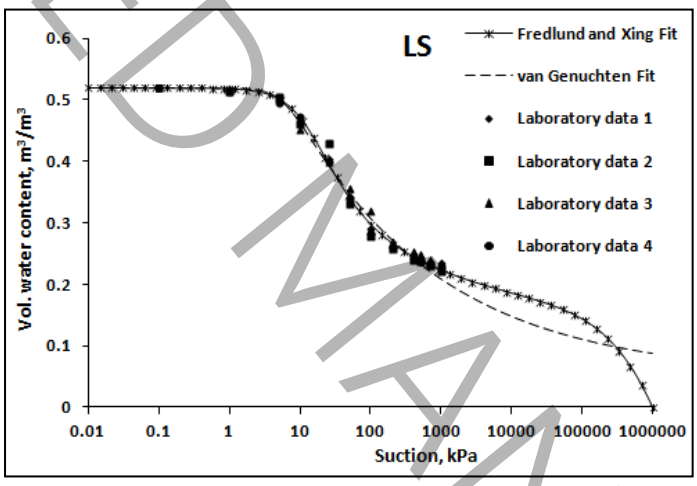

Fig. 13. SWCCS of van Genuchten, Fredlund - Xing, and experimental data: LS

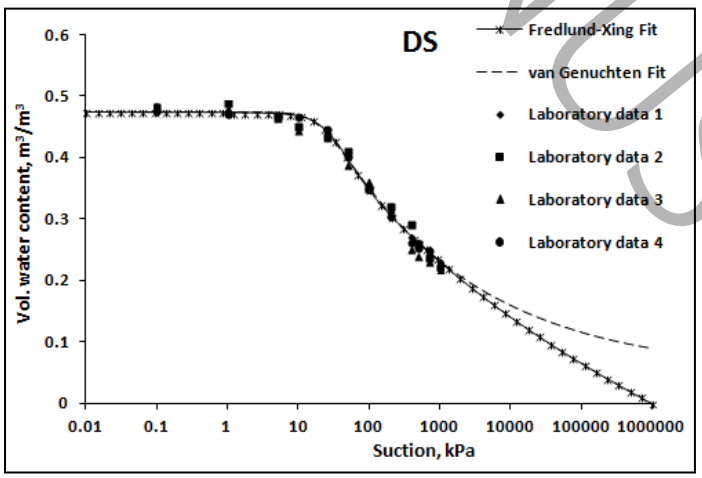

Fig. 14. SWCCS of Van Genuchten, Fredlund - Xing, and experimental data: DS

Table 5. SWCC parameters for LS and DS soils

SWCC parameters	LS			DS		
	Lab data	van Genuchten fitting	Fredlund & Xing fitting	Lab data	van Genuchten fitting	Fredlund & Xing fitting
θ_s(%)	51.9	51.9	51.9	47.4	47.4	47.4
s_{ae}(kPa)	11	6.66	9.57	20	15.3	18.96
θ_r(%)	27.6	10	29.2	29	10	28.7
(R^2)	-	0.9906	0.9977	-	0.9966	0.9993
Fitting parameters	-	b = 0.12 kPa^{-1} p = 3.0 q =0 .08	a = 15.1 kPa n = 2.3 m = 0.39	-	b = 0.17 kPa^{-1} p = 2.75 q = 0.077	a = 11.1 kPa n = 1.7 m = 0.42

R^2: Coefficient of determination

3. Conclusion

The experimental results showed that the loose soil (LS) with loose compaction and higher pore volume maintains higher capacity of water in saturation condition (52%) in comparison to the dense soil (DS) (47.4%) with a dense compaction and less pore volume. DS with lower initial void ratio and density yielded higher level of air-entry (s_{ae}) value and residual degree of saturation compared to LS with higher initial void ratio and density. Large inter-particles pores result in higher saturated conductivity allowing water to easily drain out from the soil. Hence, s_{ae} of the LS soil found to be lower than s_{ae} of the DS soil with higher hydraulic conductivity. On the other hand, air entry value increased with increasing density.

Numerical simulation was employed to verify the experimental results obtained from the modified oedometer in unsaturated condition. The analysis showed a similarity of about 95% to 97% between experimental and numerical methods.

The laboratory experimental curve developed using the equation of Fredlund and Xing was almost perfectly line on the laboratory data especially at high suction pressure (more than 100 kPa). The air entry values of Fredlund and Xing fitting were very close to the air entry values obtained from laboratory data

for the LS and DS soils. Regarding residual water content, the Fredlund and Xing values (29.2 and 28.7 kPa) are also more reasonable compared to the value of Van Genuchten. The empirical equation suggested by Fredlund and Xing was modified to describe relationship of SWCC of the granite residual soil as it fitted well with the experimental results.

4. References

[1] Aziz, A.A., Ali, F.H., Heng, C.F., Mohammed, T.A. and Huat, B.B.K., Collapsibility and volume change behavior of unsaturated residual soil, 2005.

[2] Huat, B.B.K., Aziz, A.A., Ali, F.H., Faisal, F.H., and Azmi N.A., Effect of Wetting on Collapsibility and Shear Strength of Tropical Residual Soils. Electronic Journal of Geotechnical Engineering, 13(G) (2008) 1-14.

[3] Hilf, J.W., An investigation of pore-water pressure in compacted cohesive soils. Ph.D. thesis, Technical Memorandum 654, U.S. Department of the Interior Bureau of Reclamation, Denver, Colorado, 1956.

[4] Ke, C., Wen-gui, C., He, C., Hysteresis incremental model of soil-water characteristic curve based on pore expansion and contraction, Rock and Soil Mechanics, 41(10) (2020) 3236-3244.

[5] Chen, W-w., Jia, Q-q., Tong, Y-m., Measurement and curve fitting for the soil-waterer characteristic curve of mural plaster at Mogao Grottoes, Rock and Soil Mechanics, 41(5) (2020) 1483-1491.

[6] Vanapalli, S.K., Fredlund, D.G., Pufahl, D.E. and Clifton, A.W. (1996). Model for the prediction of shear strength with respect to soil suction, Canadian Geotechnical Journal. 33(3): 379–392.

[7] Balighi, M., Baradaran, M.S., Akhtarpour, A., Numerical investigation of swelling soil behavior and its effect on gas well casing internal forces based on unsaturated soil mechanics, case study: Khangiran, Sarakhs, Amirkabir Journal of Civil Engineering, 56(7) (2024) 885-908.

[8] Douzali Joushin1, F., Badv, K., Barin, M., Soltani Jigheh, H., Prediction of the soil-water characteristic curve of dune sand stabilized with SBR polymer and MICP process in the Jabal Kandi area, Journal of Engineering Geology, 4 (13) (2020) 4-7.

[9] Fredlund, D.G. and Xing, A., Equations for soil-water characteristic curve, Canadian Geotechnical Journal. 31(1994) 521-532.

[10] Van Genuchten, M.T., A closed form equation for predicting the hydraulic conductivity of unsaturated soils. Soil Science Society of America Journal. 44(5) (1980) 892–898.

[11] Leong, E-C., Soil-water characteristic curves – Determination, estimation and application, 7th Asia-Pacific Conference on Unsaturated Soils, Japanese Geotechnical Society Special Publication, Japanese Geotechnical Society Special Publication, 7(2) (2019) 21-30.

[12] Seki, K., Toride, N., & Th. van Genuchten, M., Closed-form hydraulic conductivity equations for multimodal unsaturated soil hydraulic properties. Vadose Zone Journal. 21 (2022).

[13] Guellouz, L., Askri, B., Jaffré, J., Bouhlila, R., Estimation of the soil hydraulic properties from field data by solving an inverse problem. Scientific Reports. 10(1) (2020).

[14] Kholghifard, M., Ahmad, K., Kassim, A., Ali, N., Kalatehjari, R., Babakanpour, F., Temperature effect on compression and collapsibility of residual granitic soil, GRADEVINAR, 66(03) (2014) 191-196.

[15] Kholghifard, M., Ahmad, K., Kassim, A., Ali, N., Kalatehjari, R., Collapse/Swell Potential of Residual Laterite Soil Due to Wetting and Drying-wetting Cycles. National Academy Science Letters, 37(2) (2014) 147–153.

[16] Kholghifard, M., Ahmad, K. Effect of Matric Suction and Density on Yield Stress, Compression Index and Collapse Potential of Unsaturated Granite Soil. KSCE J Civ Eng, 25 (2021), 2847–2854.

[17] D ASTM, D-6836−02, Standard test method for soil water characteristic curve for desorption using pressure extractor. Philadelphia: ASTM standards, Reapproved 2008.

[18] ELE International, ELE Geotechnical Software package, DS7. Milton Keynes, United Kingdom: ELE International; 2007.

[19] Fredlund, D.G. and Rahardjo, H., Soil Mechanics for Unsaturated Soils. New York: John Wiley & Sons, 1993.

[20] Toll, D.G., A conceptual model for the drying and wetting of soil. Proceeding of the 1st International Conference on Unsaturated soils, Paris, France, (1995) 805-810.

[21] Geo-Slope International Ltd., An Engineering Methodology: SEEP/W and AIR/W). 4th edition, Alberta, Canada, Geo-Sope International Ltd, 2009.

[22] Kawai, K., Karube, D. and Kato, S., The Model of Water Retention Curve Considering Effects of Void Ratio. In Rahardjo, H., Toll, D.G., Leong, E.C. (Eds.), Unsaturated Soils for Asia, Rotterdam Balkema, (2000) 329-334.

[23] Lins, Y., Hydro-Mechanical Properties of Partially Saturated Sand. Faculty of Civil Engineering, University Bochum, Weibenfels, Germany, 2009.

[24] Abedi Koupai, J., Pourabdollah, N., Ansari, S., Estimation of soil water characteristic curve parameters in differentmodels in light soils, Journal of New Approaches in Water Engineering and Environment, 3(1) (2024) 136-148.

[25] Tabana, A., Mirmohammad Sadeghib, M., and Rowshanzamir, M.A., Estimation of van Genuchten SWCC model for unsaturated sands by means of the genetic programming, Scientia Iranica, Transactions A: Civil Engineering, 25 (2018) 2026-2038.

[26] Niu, G., Kong, L., Miao, Y., Li, X., Chen, F. A., A Modified Method for the Fredlund and Xing (FX) Model of Soil-Water Retention Curves, Processes, 2024, 12, 50.

[27] Mahmood, M.S., Abrahim, M.J., and Saleh, S.M., Reliability assessment of the soil-ater-retention for unsaturated sand soils, Kufa Journal of Engineering, 16(1) (2025) 1-12.

[28] Zhai Q., Rahardjo H., Satyanaga, A., Effects of residual suction and residual water content on the estimation of permeability function. Geoderma, 303 (2017) 165-177.